



HAL
open science

Oxidation dependence of the Dzyaloshinskii-Moriya interaction in Pt/Co/MO_x trilayers (M=Al or Gd)

Dayane de Souza Chaves, Fernando Ajejas, Viola Křížáková, Jan Vogel,
Stefania Pizzini

► **To cite this version:**

Dayane de Souza Chaves, Fernando Ajejas, Viola Křížáková, Jan Vogel, Stefania Pizzini. Oxidation dependence of the Dzyaloshinskii-Moriya interaction in Pt/Co/MO_x trilayers (M=Al or Gd). *Physical Review B*, 2019, 99 (14), pp.144404. 10.1103/PhysRevB.99.144404 . hal-01582132

HAL Id: hal-01582132

<https://hal.science/hal-01582132>

Submitted on 24 Aug 2023

HAL is a multi-disciplinary open access archive for the deposit and dissemination of scientific research documents, whether they are published or not. The documents may come from teaching and research institutions in France or abroad, or from public or private research centers.

L'archive ouverte pluridisciplinaire **HAL**, est destinée au dépôt et à la diffusion de documents scientifiques de niveau recherche, publiés ou non, émanant des établissements d'enseignement et de recherche français ou étrangers, des laboratoires publics ou privés.

Oxidation dependence of the Dzyaloshinskii-Moriya interaction in Pt/Co/ MO_x trilayers ($M = \text{Al}$ or Gd)

Dayane de Souza Chaves,¹ Fernando Ajejas,^{2,*} Viola Křížáková,¹ Jan Vogel,¹ and Stefania Pizzini^{1,†}

¹*Université Grenoble Alpes, CNRS, Institut Néel, F-38000 Grenoble, France*

²*Universidad Autónoma de Madrid Campus de Cantoblanco, 28049 Madrid, Spain*



(Received 29 August 2017; revised manuscript received 19 January 2019; published 4 April 2019)

We have studied the interfacial Dzyaloshinskii-Moriya interaction (DMI) in Pt/Co/ MO_x ($M = \text{Al}, \text{Gd}$) trilayers in which the degree of oxidation of the top Co interface is varied. To access reliable values of the DMI strength, we have used a method based on the measurement of the saturation velocity of field driven chiral Néel domain walls. We show that the effective DMI strength in the Pt/Co/ MO_x trilayers varies with the oxidation degree of the Co/ MO_x interface. This strongly suggests that the Co/ MO_x interface gives a distinct contribution to the total DMI, adding to that of the Pt/Co interface. The DMI presents a maximum for the oxygen coverage maximizing also the interface magnetic anisotropy energy K_x . This calls for common microscopic origins for the contributions of the Co/ MO_x interface to DMI and K_x .

DOI: [10.1103/PhysRevB.99.144404](https://doi.org/10.1103/PhysRevB.99.144404)

I. INTRODUCTION

In the last few years, the study of magnetic multilayers has known a strong revival, following the discovery that the interfacial Dzyaloshinskii-Moriya interaction (DMI) [1,2] may become non-negligible with respect to the Heisenberg exchange and lead to nontrivial magnetic configurations. In ultrathin ferromagnetic (FM) layers in contact with a heavy metal (HM) with large spin-orbit coupling (SOC) within a noncentrosymmetric stack, the interfacial DMI may lead to the stabilization of chiral magnetic textures such as chiral Néel walls [3] and magnetic skyrmions [4,5]. The chirality of the spin configuration introduces interesting features of the magnetization dynamics. Large DMI stabilizes the domain wall (DW) internal structure against precession [3], so that DWs can be driven to very large velocities by magnetic fields [6–8]. Moreover, chiral Néel walls and skyrmions can be displaced efficiently via spin-orbit torques when driven by electrical currents [5,9,10]. Routes to optimize the DMI are therefore targeted, as both kinds of magnetic textures are forecast to become carriers of binary information in future spintronic devices, like racetrack memories [11,12].

The understanding of the microscopic mechanisms leading to interfacial DMI—and therefore to chiral magnetic textures—is still elusive, and little is known about the relation between the DMI and the details of the electronic structure. The DMI was introduced as a superexchange term in low-symmetry crystals [1,2], and later extended to metals [13]. In 1990 Fert showed with an analytical model that the DMI term is allowed also in thin films due to the symmetry reduction at the interfaces [14]. At FM/HM interfaces the superexchange

between FM spins is mediated by the heavy metal atoms and the DMI strength is expected to scale with the HM spin-orbit coupling. Recently, a few groups have developed density functional theory (DFT) calculations to address quantitatively the DMI in several HM/FM bilayer systems [15–17] and models to predict the variation of the DMI for $3d/5d$ interfaces have been proposed [17,18]. Such calculations can guide experimentalists towards the optimization of materials with large DMI, although they consider ideal interfaces, while experiments concentrate on multilayer systems grown by magnetron sputtering, where polycrystallinity and interfacial roughness can influence the strength and even the sign of the DMI [19]. Experimental techniques to measure DMI are based on the nonreciprocal dispersion of spin waves within the FM layers [20–23], on the anisotropic propagation of chiral Néel walls [24–27], or on chiral nucleation of reversed domains [28]. Recently, we have proposed a method to extract the DMI strength from the saturation velocity of field-driven domain walls [8,29].

Among the many systems with DMI, the Pt/Co interface is the most studied, following the original work by Miron *et al.* that found very large current-driven domain-wall velocities in Pt/Co/ AlO_x trilayers [30]. *Ab initio* [15,16,31] and experimental studies on polycrystalline stacks [21,22,28,32] agree on the fact that this interface is the source of strong DMI favoring homochiral magnetic textures (chiral Néel walls and skyrmions) with anticlockwise rotation of the magnetic moments.

The contribution of the FM/oxide interface to the total (effective) DMI in HM/FM/ MO_x trilayers is also a subject of interest, as the absence of strong SOC calls for a new microscopic mechanism. Recent *ab initio* calculations have predicted that the sign and the strength of the DMI in Ir/Fe/O trilayers can be tuned by varying the oxygen coverage of the Fe layer [33]. Similar results are anticipated in the case of any electronegative atom covering the cobalt layer and this

*Present address: Unité Mixte de Recherche CNRS-Thales, Université Paris-Saclay, Palaiseau, France.

†stefania.pizzini@neel.cnrs.fr

suggests that the DMI could be electrically tuned, as observed recently for Ta/CoFeB/TaO_x [34]. Strong DMI contributions were predicted for Co/O [15,31,35] and Co/C [36] interfaces. The modification of the 3*d* band structure at the Fermi level [33] or a Rashba-type DMI have been invoked [31,36]. The large DMI measured in Pt/Co/MgO has been attributed to the presence of DMI at the Co/O interface [35]. On the other hand, the small DMI measured for Pt/Co/graphene stacks has been interpreted as coming from DMI at the Co/*gr* interface, having opposite sign as that of the Pt/Co interface [37]. However a clear demonstration of the presence of DMI at the Co/O interface is still elusive, as it is not straightforward to separate experimentally the DMI contributions coming from the bottom and top FM interfaces in a trilayer system.

In this paper, we report the study of interfacial DMI in a series of Pt/Co/MO_x samples in which the degree of oxidation of the top Co interface is varied. We show that the effective DMI strength in the Pt/Co/MO_x trilayers varies with the oxidation degree of the cobalt layer, suggesting that the Co/MO_x interface gives a distinct contribution to the total DMI, adding to that of the Pt/Co interface. The DMI presents a maximum for the condition where the interface magnetic anisotropy energy is also maximum, calling for common microscopic origins for the contributions of the Co/MO_x interface to DMI and K_s .

II. MAGNETIC CHARACTERIZATIONS

Measurements were carried out on Pt(30)/Co(0.8)/AlO_x (1–3)/Pt(2) and Pt(4)/Co(1)/GdO_x(1–3)/Al(3) stacks (thickness in nm). All samples were grown by magnetron sputtering at room temperature on 8-cm-long Si/SiO₂ substrates. By choosing an off-axis geometry between target and substrate, the Al and Gd layers were grown in the shape of a wedge with a thickness gradient and then exposed to an oxygen plasma. The thickness gradient results in an increasing oxidation of the top part of the Co layer, going from the thicker to the thinner Al (Gd) layers [see sketch in Fig. 1(a)]. The magnetic properties of the two samples were obtained from vibrating-sample magnetometer–superconducting quantum interference

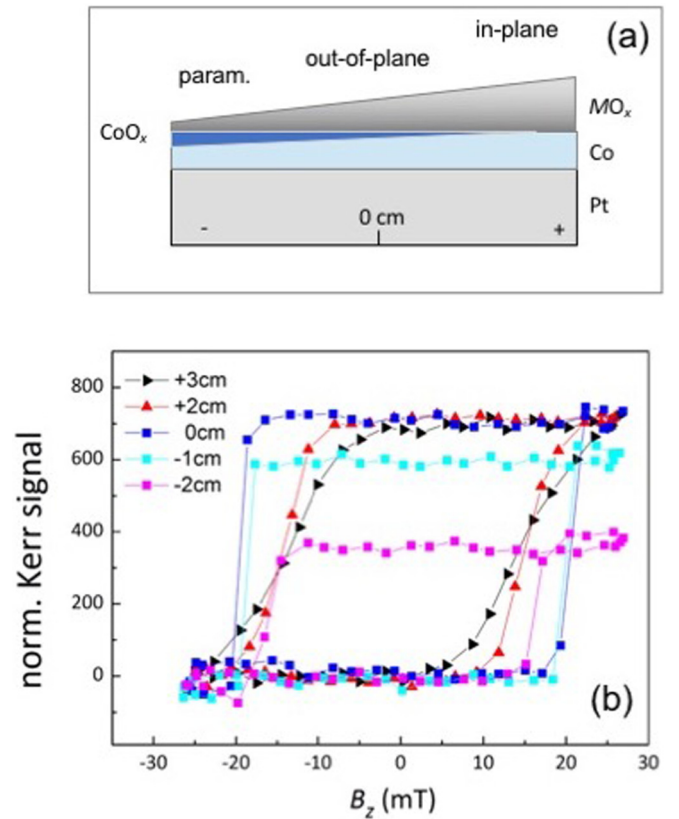


FIG. 1. (a) Sketch of the sample stacks: the Al (Gd) layer thickness increases going from negative to positive x positions. After oxygen plasma, the gradient of Al (Gd) thickness results in a gradient of oxidation of the Co layer; (b) hysteresis loops measured by magneto-optical Kerr effect in different positions of the Pt/Co/AlO_x wedge.

device (VSM-SQUID) measurements and magneto-optical Kerr microscopy in different positions of the wedge. The unit surface magnetization $M_s t$ (t being the thickness of the unoxidized Co layer) and the in-plane saturation field $\mu_0 H_K$

TABLE I. Unit surface magnetization $M_s t$, effective anisotropy field $\mu_0 H_K$, saturation domain-wall speed v_{\max} , DMI field $\mu_0 H_{\text{DMI}}$, interface DMI energy density D_s extracted from v_{\max} and from $\mu_0 H_{\text{DMI}}$, for some selected positions along the two wedged samples.

Sample	x (cm)	$M_s t$ (10^{-3} A)	$\mu_0 H_K$ (T)	v_{\max} (m/s)	$\mu_0 H_{\text{DMI}}$ (mT)	D_s^{\max} (pJ/m)	D_s^{DMI} (pJ/m)
Pt/Co/AlO _x	-2	0.5 ± 0.1	1.8 ± 0.1	410 ± 20		0.8 ± 0.1	
	-1.5	0.7	1.75			1.06	
	-1	0.9	1.52	440		1.43	
	0	1.3	0.90	310		1.42	
	+1	1.4	0.53	240		1.22	
	+2	1.5	0.23				
Pt/Co/GdO _x	-3.5	0.68	1.62	255	> 260	0.62	0.6 ± 0.2
	-2	0.93	1.24	330	260	1.11	1.04
	-1	0.97	1.05	320	220	1.08	1.02
	0	1.12	0.62	315	190	1.34	1.42
	+1	1.12	0.74	300	150	1.29	1.02
	+1.5	1.11	0.77	270	170	1.12	0.98

are reported in Table I (see also Fig. 4). The hysteresis loops measured by polar Kerr microscopy for the Pt/Co/AlO_x are shown in Fig. 1(b). Within the region studied in this work, the magnetization of both Pt/Co/AlO_x and Pt/Co/GdO_x is out of plane. In the under-oxidized part of the sample (thick AlO_x or GdO_x), the magnetization is in plane. Going towards thinner AlO_x or GdO_x layers, the unit surface magnetization decreases, as the Co layer becomes more and more oxidized. This is also shown by the hysteresis loops, where the decrease of the Kerr signal is related to the decrease of the magnetic Co thickness. X-ray reflectivity (XRR) data indicate that for the thinnest AlO_x (or GdO_x) layers studied here, the Co layers are oxidized over ~0.3 nm. VSM-SQUID measurements carried out at low temperature show that the thin oxide layer does not induce exchange bias and that the Curie temperature is well above room temperature even for the most oxidized part of the Co layer.

For both Pt/Co/MO_x wedge samples, $M_s t$ is larger (with a plateau) on the thick MO_x side and decreases on the thinner side, as the Co layer gets more and more oxidized. The interface magnetic anisotropy K_s also depends on the wedge position (see Fig. 4). The maximum of K_s is observed for an intermediate Al or Gd layer thicknesses, where $M_s t$ is still at its maximum value or starts decreasing due to the onset of oxidation. These results are in agreement with those previously reported for Pt/Co/AlO_x samples in which the perpendicular magnetic anisotropy (PMA) was optimized by tuning the degree of oxidation of the top Co interface [38–41]. Our x-ray photoelectron spectroscopy study [38,39] showed that the onset of PMA is related to the appearance of a significant density of Co-O bonds at the Co/AlO_x interface. Moreover, the PMA was shown to be maximized when the top Co interface is completely covered by oxygen atoms. The oxidation dependence of the PMA was observed for several oxides covering Pt/Co bilayers [42]. These works proved that the oxidation of the top Co interface gives rise to an anisotropy term that adds to that present at the Pt/Co interface. Based on these results, we correlate the maximum PMA in our wedge samples to the optimum oxidation degree of the Co layer, realized for intermediate Al (Gd) thicknesses.

III. DOMAIN-WALL VELOCITY AND DMI STRENGTH

The strength and the sign of the DMI was addressed with two methods based on the measurement of domain-wall velocity, using wide field magneto-optical Kerr microscopy. The film magnetization was first saturated in the out-of-plane direction. An opposite magnetic field pulse B_z was then applied to nucleate one or several reverse domains. Using a 200- μm -diameter coil associated to a fast current source, out-of-plane magnetic field pulses of strength up to $B_z = 700$ mT and duration down to 20 ns could be applied. The DW velocities were deduced from the expansion of the initial bubble domain, after the application of further magnetic field pulses (see an example in Fig. 3).

The first method relies on the measurement of the DW speed as a function of the easy-axis field magnitude B_z . It was recently shown [6–8,29] that in multilayers with strong DMI the field-driven DW speeds largely exceed those obtained in symmetric systems for the same fields [8,43] and that, contrary to what is predicted by one-dimensional (1D) micromagnetic simulations, the speed does not decrease after the Walker field. Instead, the DW speed reaches a plateau that can extend up to very large fields. We have demonstrated [8,29] that the saturation DW speed can be related to the DMI strength via the expression

$$v_{\text{sat}} = \frac{\pi}{2} \gamma \frac{D}{M_s}, \quad (1)$$

where D is the DMI strength, M_s is the spontaneous magnetization, and γ is the gyromagnetic ratio. This implies that the measurement of the saturation speed, together with that of M_s , provides a simple way to obtain the strength of the effective DMI interaction in a trilayer system. This approach was validated quantitatively by 2D micromagnetic simulations and some of the results are presented in Ref. [8]. Since the DMI in these layers has an interface origin, we find it more appropriate to derive the interfacial DMI strength D_s from our experiments, so that

$$D_s = D t = 2 v_{\text{sat}} \frac{M_s t}{\pi \gamma}. \quad (2)$$

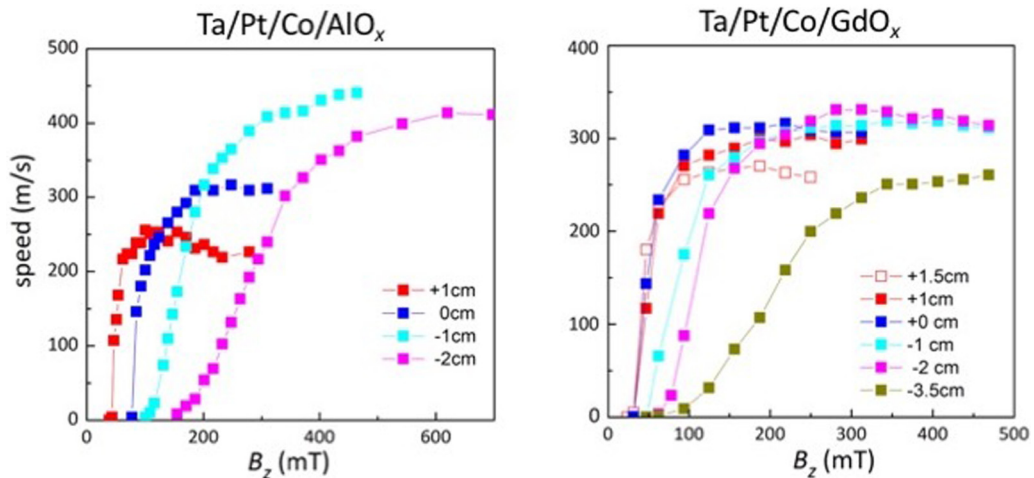


FIG. 2. DW speed as a function of out-of-plane field B_z for Pt/Co/AlO_x and Pt/Co/GdO_x for different wedge positions reflecting different oxidation degrees of the Co layer.

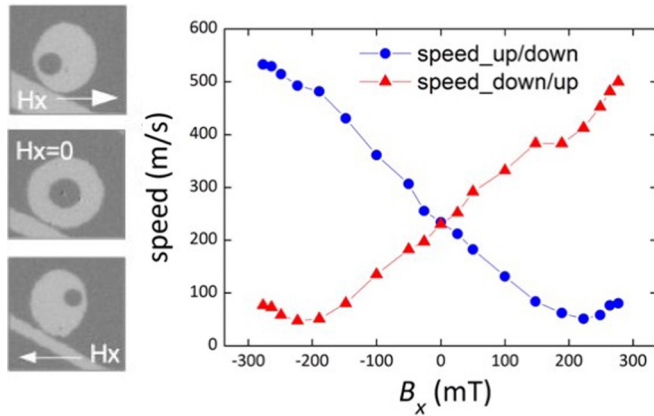


FIG. 3. DW speed vs in-plane magnetic field B_x , measured for up/down and down/up DW propagating in $\pm x$ direction, driven by 30-ns-long B_z pulses of 80 mT, for the Pt/Co/GdO_x sample in position +0.5 cm. The differential Kerr images represent the expansion of a bubble domain driven by B_z pulses with constant $B_x = -120, 0,$ and $+120$ mT.

The determination of D_s is more reliable than that of D , as it is related to $M_s t$, that can be measured precisely, rather than M_s that requires the exact thickness t of the ultrathin ferromagnetic layer.

The DW velocity curves, measured for several positions of the AlO_x and GdO_x wedge, are shown in Figs. 2(a) and 2(b). The curves present the features described above, with the saturation velocities ranging from 200 to 400 m/s and a plateau of velocity extending up to 500 mT. These features suggest large DMI values. The interfacial DMI strength determined using Eq. (2) are reported in Table I and in Fig. 4.

Since the saturation speed is independent of the DMI sign, the sign of the DMI was obtained using the method proposed by Je *et al.* [24] and used in our previous studies [8,27]. This consists in measuring the domain-wall propagation by an out-of-plane field, in the presence of a constant in-plane magnetic field B_x parallel to the DW normal. In systems with DMI and chiral Néel walls, the DW propagation is anisotropic in the direction of B_x and the DW speed is larger/smaller for the domain walls having magnetization parallel/antiparallel to the in-plane field (Fig. 3). Using this approach, we found that in all our samples the DMI stabilizes anticlockwise spin rotation within the DWs (negative D values). When the DW speed is measured as a function of the in-plane magnetic field strength, it can be shown that it reaches a minimum when H_x compensates the H_{DMI} field that pins the DWs in the Néel configuration. We can then deduce the average DMI energy density D , since $H_{\text{DMI}} = D/\mu_0 M_s \Delta$ where $\Delta = \sqrt{A/K_0}$, A is the exchange stiffness, and K_0 is the effective anisotropy energy.

For some of the samples, we have compared the DMI values extracted from Eq. (2) to those obtained from the method just described. The B_z field driving the DWs was chosen to be beyond the depinning field, so that the complications shown to occur in the creep regime were avoided [27]. Note that this method presents the disadvantage of requiring the value of the exchange stiffness of the Co layer, a parameter that is in general difficult to evaluate in ultrathin films. In

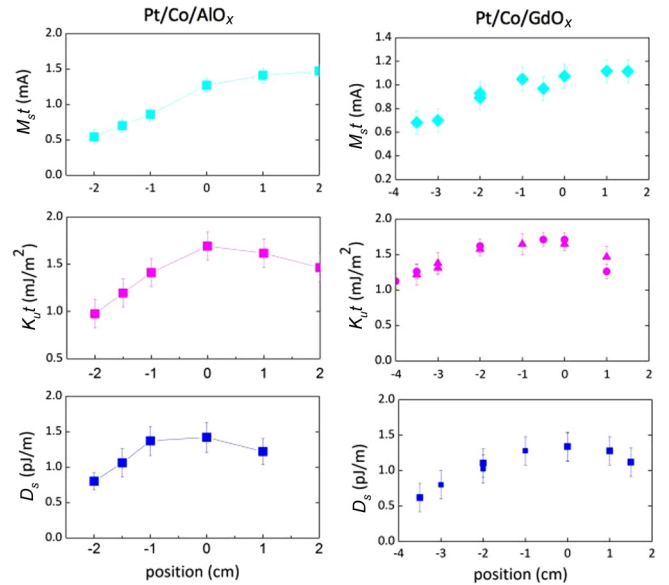


FIG. 4. Unit surface magnetization $M_s t$, interface magnetic anisotropy energy $K_u t$, and interfacial DMI strength D_s measured as a function of wedge position (i.e., of oxidation) for the Pt/Co/AlO_x (left) and the Pt/Co/GdO_x wedge sample (right).

this study we have used $A = 16$ pJ/m, the value for which in our previous work on similar samples we found the best agreement with the DMI values measured by Brillouin light scattering [8]. The results reported in Table I show that for all the MO_x wedge positions, the DMI values obtained with the two methods differ by less than $\sim 15\%$. By comparing the DMI obtained with the two methods, our method provides a simple way to evaluate the exchange stiffness of the magnetic layer in which the DWs propagate. Our results also indicate that in our systems the exchange stiffness does not change significantly with the thickness of the Co layer as it gets more and more oxidized, since the agreement between the values of M_s obtained with the two methods stays good keeping a constant value of A .

In Fig. 4, the interfacial DMI strength measured along the AlO_x and GdO_x wedges is plotted together with the variation of the unit surface magnetization $M_s t$ and the interface anisotropy energy density.

IV. DISCUSSION

The main result of this work is that in Pt/Co/MO_x samples the interface DMI strength changes with the degree of oxidation of the top Co layer, and reaches a maximum where the perpendicular magnetic anisotropy is also the largest (see Fig. 4). Since the Pt/Co interface remains unchanged along the wedge (from XRR measurements, the largest oxide thickness is only 0.3 nm thick for a nominal Co thickness of 0.8–1 nm), the variation of the interface DMI can be ascribed to the modification of the top Co interface only. In both Pt/Co/AlO_x and Pt/Co/GdO_x samples, while the oxidation degree of the Co layer changes continuously along the wedge, the DMI strength changes in a *nonmonotonous* way. This is also the case for the variation of the PMA, that is correlated with the

varying oxidation degree of the Co layer, as discussed above. Therefore, the optimum Co oxidation not only determines the maximum interface anisotropy but also optimizes the interfacial DMI. This invokes similar microscopic mechanisms for the variation of K_i and DMI.

Some recent theoretical works invoke the presence of DMI at the interface between a ferromagnetic layer (Co or Fe) and an electronegative atom (oxygen or carbon). The DFT calculations of Belabbes *et al.* [33] consider the case of Ir(001)/Fe(1 ML)/O and show that the DMI can be tuned by controlling the oxygen coverage. In this extreme case where the FM is only 1 ML thick and the FM layer cannot be seen as having two separate interfaces, it is shown that the DMI strength and sign are controlled by the hybridization of the Co-3*d* and HM-5*d* electronic bands [17,33]. The charge transfer between Co and O, observed for example by Daalderop *et al.* [44] can modify the Co-HM distances and modify the 3*d*-5*d* hybridization, therefore changing the 3*d* density of states at the Fermi level and the DMI.

The *ab initio* calculations in Ref. [35] consider a Pt(111)/Co(3 ML)/MgO trilayer. The layer resolved calculations show that although the main contribution to the DMI is situated at the Pt/Co interface, a significant DMI is also present at the Co/O interface. The latter DMI has the same sign as that of the Pt/Co interface and therefore enhances the total DMI. This study considering a 3-ML-thick FM layer has to be distinguished from [33] in the sense that the oxygen coverage does not simply leverage a change of the DMI at the HM/FM interface by modifying the electronic structure, but also promotes a (separate) DMI contribution centered at the Co/O interface.

In the systems studied here, where the Co layers are thicker than 3 ML, the Pt/Co and Co/ MO_x interfaces can then be considered as contributing independently to the DMI. We then attribute the variation of the total DMI as a function of wedge position (i.e., of Co oxidation) to a DMI contribution located at the Co/O interface, whose strength varies and reaches a maximum for the optimum oxidation. This conclusion is in line with the first-principle calculations of [45] that studied the variation of the PMA of a Fe/MgO (and Co/MgO) bilayer for different oxidation degrees of the Fe (Co) interface. Despite the weak spin-orbit interaction at FM/O interfaces, the oxidation was shown to play an essential role in the PMA. In that work, the maximum anisotropy was obtained for the oxygen-

terminated interfaces, while the PMA decreased for over- or under-oxidized interfaces. The origin of PMA was attributed to the overlap between O- p_z and transition metal 3*d* orbitals (optimized for O atoms on top of the FM) that give stronger spin-orbit coupling-induced splitting around the Fermi level for perpendicular magnetization orientation. The DMI energy term localized at the Co/O interface cannot be described by the Levy-Fert three-site model [14], because of the weak SOC of the scattering (oxygen) atoms. Recently, it has been predicted that at FM/insulator interfaces a contribution to the DMI might arise from the Rashba field, and its strength has been related to the Rashba coefficient [46]. At the same time, the analytical model developed by Barnes *et al.* [47] suggests that the Rashba field arising from the internal electric field in the surface region of an ultrathin ferromagnet in contact with an insulator can make an important contribution to the perpendicular magnetic anisotropy. The presence of a Rashba field at the Co/ MO_x interface, suggested in Ref. [48] for Pt/Co/ AlO_x , can then be at the origin of a PMA and a DMI term in Pt/Co/ MO_x samples, and can explain that similar variations of PMA and DMI with Co oxidation are observed in our samples.

In conclusion, we have shown experimentally that in Pt/Co/ AlO_x and Pt/Co/ GdO_x samples the Co/O interface is the source of a DMI contribution, adding to that of the Pt/Co interface, and that can be optimized, like the PMA, by tuning the oxidation of the Co/ MO_x interface. The microscopic origin of such effect is probably found in the presence of a Rashba field at the Co/O interface, that also tunes the PMA. We can anticipate that in these Pt/Co/ MO_x trilayers the DMI may be manipulated with the application of an electric field, as already observed in Ta/CoFeB/ TaO_x [34]. This may provide a smart way to engineer future spin-orbitronic devices for controllable chiral domain walls or skyrmion dynamics.

ACKNOWLEDGMENTS

S.P. and J.V. acknowledge the support of the Agence Nationale de la Recherche, Project No. ANR-17-CE24-0025 (TOPSKY). B. Fernandez, Ph. David and E. Mossang are acknowledged for their technical help. D.S.C. was supported by a CNPq Scholarship (Brazil). S.P. thanks A. Thiaville, C. Lacroix and Mairbek Chshiev for fruitful discussions.

-
- [1] I. E. Dzialoshinskii, *Sov. Phys. JETP* **5**, 1259 (1957).
 - [2] T. Moriya, *Phys. Rev.* **120**, 91 (1960).
 - [3] A. Thiaville, S. Rohart, E. Jué, V. Cros, and A. Fert, *Europhys. Lett.* **100**, 57002 (2012).
 - [4] T. Skyrme, *Nucl. Phys.* **31**, 556 (1962).
 - [5] A. Fert, V. Cros, and N. Reyren, *Nat. Rev. Mater.* **2**, 17031 (2017).
 - [6] Y. Yoshimura, K.-J. Kim, T. Taniguchi, T. Tono, K. Ueda, R. Hiramatsu, T. Moriyama, N. Yamada, Y. Nakatani, and T. Ono, *Nat. Phys.* **12**, 157 (2016).
 - [7] K. Yamada and Y. Nakatani, *Appl. Phys. Express* **8**, 093004 (2015).
 - [8] T. H. Pham, J. Vogel, J. Sampaio, M. Vaňatka, J.-C. Rojas-Sanchez, M. Bonfim, D. S. Chaves, F. Choueikani, P. Ohresser, E. Otero, A. Thiaville, and S. Pizzini, *Europhys. Lett.* **113**, 67001 (2016).
 - [9] S. Emori, U. Bauer, S.-M. Ahn, E. Martinez, and G. Beach, *Nat. Mater.* **12**, 611 (2013).
 - [10] K.-S. Ryu, L. Thomas, S.-H. Yang, and S. Parkin, *Nat. Nanotechnol.* **8**, 527 (2013).
 - [11] S. Parkin, M. Hayashi, and L. Thomas, *Science* **320**, 190 (2008).
 - [12] A. Fert, V. Cros, and J. Sampaio, *Nat. Nanotechnol.* **8**, 152 (2013).
 - [13] A. Fert and P. M. Levy, *Phys. Rev. Lett.* **44**, 1538 (1980).

- [14] A. Fert, *Mater. Sci. Forum* **59-60**, 439 (1990).
- [15] F. Freimuth, S. Blügel, and Y. Mokrousov, *J. Phys.: Condens. Matter* **26**, 104202 (2014).
- [16] H. Yang, A. Thiaville, S. Rohart, A. Fert, and M. Chshiev, *Phys. Rev. Lett.* **115**, 267210 (2015).
- [17] A. Belabbes, G. Bihlmayer, F. Bechstedt, S. Blügel, and A. Manchon, *Phys. Rev. Lett.* **117**, 247202 (2016).
- [18] V. Kashid, T. Schena, B. Zimmermann, Y. Mokrousov, S. Blügel, V. Shah, and H. G. Salunke, *Phys. Rev. B* **90**, 054412 (2014).
- [19] A. W. J. Wells, P. M. Shepley, C. H. Marrows, and T. A. Moore, *Phys. Rev. B* **95**, 054428 (2017).
- [20] K. Di, V. L. Zhang, H. S. Lim, S. C. Ng, M. H. Kuok, J. Yu, J. Yoon, X. Qiu, and H. Yang, *Phys. Rev. Lett.* **114**, 047201 (2015).
- [21] M. Belmeguenai, J.-P. Adam, Y. Roussigné, S. Eimer, T. Devolder, J.-V. Kim, S. M. Cherif, A. Stashkevich, and A. Thiaville, *Phys. Rev. B* **91**, 180405(R) (2015).
- [22] J. Cho, N.-H. Kim, S. Lee, J.-S. Kim, R. Lavrijsen, A. Solignac, Y. Yin, D.-S. Han, N. J. J. van Hoof, H. J. M. Swagten, B. Koopmans, and C.-Y. You, *Nat. Commun.* **6**, 7635 (2015).
- [23] S. Tacchi, R. E. Troncoso, M. Ahlberg, G. Gubbiotti, M. Madami, J. Åkerman, and P. Landeros, *Phys. Rev. Lett.* **118**, 147201 (2017).
- [24] S.-G. Je, D.-H. Kim, S.-C. Yoo, B.-C. Min, K.-J. Lee, and S.-B. Choe, *Phys. Rev. B* **88**, 214401 (2013).
- [25] A. Hrabec, N. A. Porter, A. Wells, M. J. Benitez, G. Burnell, S. McVitie, D. McGruther, T. A. Moore, and C. H. Marrows, *Phys. Rev. B* **90**, 020402(R) (2014).
- [26] R. Lavrijsen, D. M. F. Hartmann, A. van den Brink, Y. Yin, B. Barcones, R. A. Duine, M. A. Verheijen, H. J. M. Swagten, and B. Koopmans, *Phys. Rev. B* **91**, 104414 (2015).
- [27] M. Vaňatka, J.-C. Rojas-Sánchez, J. Vogel, M. Bonfim, A. Thiaville, and S. Pizzini, *J. Phys.: Condens. Matter* **27**, 32002 (2015).
- [28] S. Pizzini, J. Vogel, S. Rohart, L. D. Buda-Prejbeanu, E. Jué, O. Boulle, I. M. Miron, C. K. Safeer, S. Auffret, G. Gaudin, and A. Thiaville, *Phys. Rev. Lett.* **113**, 047203 (2014).
- [29] F. Ajejas, V. Křížáková, D. de Souza Chaves, J. Vogel, P. Perna, R. Guerrero, A. Gudin, J. Camarero, and S. Pizzini, *Appl. Phys. Lett.* **111**, 202402 (2017).
- [30] I. M. Miron, T. Moore, H. Szabolcs, L. D. Buda-Prejbeanu, S. Auffret, B. Rodmacq, S. Pizzini, J. Vogel, M. Bonfim, A. Schuhl, and G. Gaudin, *Nat. Mater.* **10**, 419 (2011).
- [31] H. Yang, O. Boulle, V. Cros, A. Fert, and M. Chshiev, *Sci. Rep.* **8**, 12356 (2018).
- [32] N.-H. Kim, J. Jung, J. Cho, D.-S. Han, Y. Yin, J.-S. Kim, H. J. M. Swagten, and C.-Y. You, *Appl. Phys. Lett.* **108**, 142406 (2016).
- [33] A. Belabbes, G. Bihlmayer, S. Blügel, and A. Manchon, *Sci. Rep.* **6**, 24634 (2016).
- [34] T. Srivastava, M. Schott, R. Juge, V. Krizakova, M. Belmeguenai, Y. Roussigne, A. Bernard-Mantel, L. Ranno, S. Pizzini, S. Cherifi, A. Stashkevich, S. Auffret, O. Boulle, G. Gaudin, M. Chshiev, C. Baraduc, and H. Bea, *Nano Lett.* **18**, 4871 (2018).
- [35] O. Boulle, J. Vogel, H. Yang, S. Pizzini, D. de Souza Chaves, A. Locatelli, T. O. Mentas, A. Sala, L. D. Buda-Prejbeanu, O. Klein, M. Belmeguenai, Y. Roussigne, A. Stashkevich, S. M. Cherif, L. Aballe, M. Foerster, M. Chshiev, S. Auffret, I. M. Miron, and G. Gaudin, *Nat. Nanotechnol.* **11**, 449 (2016).
- [36] H. X. Yang, G. Chen, A. A. C. Cotta, A. T. N'Diaye, S. A. Nikolaev, E. A. Soares, W. A. A. Macedo, A. K. Schmid, A. Fert, and M. Chshiev, *Nat. Mater.* **17**, 605 (2018).
- [37] F. Ajejas, A. Gudín, R. Guerrero, A. Anadon Barcelona, J. Diez, L. de Melo Costa, P. Olleros, M. A. Nino, S. Pizzini, J. Vogel, M. Valvidares, P. Gargiani, M. Cabero, M. Varela, J. Camarero, R. Miranda, and P. Perna, *Nano Lett.* **18**, 5364 (2018).
- [38] A. Manchon, C. Ducruet, L. Lombard, S. Auffret, B. Rodmacq, B. Dieny, S. Pizzini, J. Vogel, V. Uhlir, M. Hochstrasser, and G. Panaccione, *J. Appl. Phys.* **104**, 043914 (2008).
- [39] A. Manchon, S. Pizzini, V. Uhlir, J. Vogel, L. Lombard, C. Ducruet, S. Auffret, B. Rodmacq, B. Dieny, M. Hochstrasser, and G. Panaccione, *J. Magn. Magn. Mater.* **320**, 1889 (2008).
- [40] S. Monso, B. Rodmacq, S. Auffret, G. Casali, F. Fettar, B. Gilles, B. Dieny, and P. Boyer, *Appl. Phys. Lett.* **80**, 4157 (2002).
- [41] B. Rodmacq, A. Manchon, C. Ducruet, S. Auffret, and B. Dieny, *Phys. Rev. B* **79**, 024423 (2009).
- [42] B. Dieny and M. Chshiev, *Rev. Mod. Phys.* **89**, 025008 (2017).
- [43] P. J. Metaxas, J. P. Jamet, A. Mougín, M. Cormier, J. Ferré, V. Baltz, B. Rodmacq, B. Dieny, and R. L. Stamps, *Phys. Rev. Lett.* **99**, 217208 (2007).
- [44] G. H. O. Daalderop, P. J. Kelly, and M. F. H. Schuurmans, *Phys. Rev. B* **50**, 9989 (1994).
- [45] H. X. Yang, M. Chshiev, B. Dieny, J. H. Lee, A. Manchon, and K. H. Shin, *Phys. Rev. B* **84**, 054401 (2011).
- [46] K.-W. Kim, H.-W. Lee, K.-J. Lee, and M. D. Stiles, *Phys. Rev. Lett.* **111**, 216601 (2013).
- [47] S. E. Barnes, J. Ieda, and S. Maekawa, *Sci. Rep.* **4**, 4105 (2014).
- [48] I. M. Miron, G. Gaudin, S. Auffret, B. Rodmacq, A. Schuhl, S. Pizzini, J. Vogel, and P. Gambardella, *Nat. Mater.* **9**, 230 (2010).